

**Temperature and stress controlled surface manipulation in Ni-Al  
nano-layers**

**Sutrakar, V.K., Roy Mahapatra, D., Melnik, R.V.N.**

**Proc. 12th Annual NSTI Nanotech Conference, Nanotech Conference  
& Expo 2009, Technical Proceedings - Nanotechnology 2009, Eds.  
Laudon, M. and Romanowicz, B., Houston, Texas, May 3-7, 2009,  
USA, CRC Press, Vol. 3, 227-230,**

**ISBN: 978-1-4398-1786-5, 2009.**

# Temperature and Stress Controlled Surface Manipulation in Ni-Al Nano-Layers

D. Roy Mahapatra<sup>1,2</sup>, Vijay Kumar Sutrar<sup>3</sup>, R.V.N. Melnik<sup>4</sup>

<sup>1</sup>Department of Aerospace Engineering, Indian Institute of Science,  
Bangalore, India 560012, [droymahapatra@aero.iisc.ernet.in](mailto:droymahapatra@aero.iisc.ernet.in)

<sup>3</sup>Mechanical Engineering Design Division, Aeronautical Development Establishment,  
Defence Research and Development Organization, New Thipasandara Post,  
Bangalore, India 560075, [vijay\\_sutrar@rediffmail.com](mailto:vijay_sutrar@rediffmail.com)

<sup>4</sup>M2Net Lab, Wilfrid Laurier University, Waterloo, ON N2L3C5, Canada, [rmelnik@wlu.ca](mailto:rmelnik@wlu.ca)

## ABSTRACT

In the present paper the effects of temperature and high strain rate loading on the formation of various surface patterns in Ni-Al nano-layers are discussed. Effects of boundary conditions on the B2→BCT phase transformation in the nano-layer are also discussed. This study is aimed at developing several interesting patterned surface structures in Ni-Al nanolayer by controlling the phase transformation temperature and mechanical loading.

**Keywords:** Ni-Al, thin film, nano-layer, phase transformation, molecular dynamic simulation, thermo-mechanical loading, quantum dot array, template.

## 1. INTRODUCTION

Quantum dot arrays with precisely controlled positions and sizes are desirable for making templates for micro- and nano-electronic devices. Numerous experimental works have shown that unguided self-assembled growth of quantum dots usually fails to realize perfectly ordered dot arrays. Recently much effort has been shifted to the usage of guided self-assembly through pre-patterning, and several pre-patterning methods have been reported, including selective epitaxial growth in oxidized windows [1], buried stress field due to ion implantation [2,3], surface roughening through cooperative island formation [2], and electron beam lithography with subsequent reactive ion etching [4]. These pre-patterned substrate surfaces are usually manifested with either ordered concave pits, or ordered convex humps, or regular strain energy profiles [5]. It is expected that at each pit or hump, a single quantum dot can form after the subsequent growth, resulting in a one pit hump - one dot relation.<sup>1</sup>

<sup>2</sup> Corresponding author. (D. Roy Mahapatra)  
Tel: + 91-80-22932419; Fax: +91-80-23600134.

In reality, quantum dots have been found to nucleate at different positions even if an ordered pre-patterned substrate is used, often failing to maintain strong correlation. Hence the method to reliably and reproducibly achieve ordered quantum dot arrays through surface pre-patterning is still not known. Furthermore, there are still many unresolved issues regarding the kinetics and thermodynamics underlying the quantum dot formation and self-assembly. In recent years, Molecular Dynamics (MD) simulations have been performed extensively and reported in published literature for material property characterizations including phase-transformation behavior at nano-scale. For example, a surface stress driven phase transformation from face-centered-cubic (FCC) to body-centered-tetragonal (BCT) has been observed in gold nanowires by Diao *et al.* [6] and from FCC to pentagon crystalline structure has been observed in Cu nanowires under high strain rate loading by the present authors [7, 8]. Novel shape memory and pseudo-elastic behavior have also been observed in single crystalline, monoatomic FCC nanowires [9, 10].

Our present study is focused on the development of several interesting patterned surface structures by controlling the phase transformation temperature and mechanical loading of a NiAl nano-layer using atomistic simulations. The effects of boundary conditions and mechanical loading on the formation of surface patterns of the nano-layer are also discussed.

## 2. MODELING AND SIMULATIONS

In the present paper, we consider NiAl nano-layer of an initial Austenite (B2) phase and results based on extensive Molecular Dynamics (MD) simulations of such B2-NiAl nano-layers by Embedded Atom Method (EAM) [11, 12] are reported. In the EAM, the total energy  $E_{\text{tot}}$  of a binary system of atoms  $A$ - $B$  is represented as

$$E_{\text{tot}} = \frac{1}{2} \sum_{ij} \phi_{\alpha_i-\alpha_j}(r_{ij}) + \sum_i F_{\alpha_i}(\bar{\rho}_i), \quad (1)$$

where  $\phi_{\alpha_i-\alpha_j}(r_{ij})$  is a pair-wise interaction potential as a function of distance  $r_{ij}$  between atom  $i$  and  $j$  that have chemical sorts  $\alpha_i$  and  $\alpha_j$  ( $A$  or  $B$ ), and  $F_{\alpha_i}$  is the embedding energy of an atom of chemical sort  $\alpha_i$  as a function of the host electron density  $\bar{\rho}_i$  induced at atom site  $i$  by all other atoms in the system. The host electron density is given by

$$\bar{\rho}_i = \sum_{j \neq i} \rho_j(r_{ij}), \quad (2)$$

where  $\rho_{\alpha_j}(r)$  is the electron density function assigned to an atom of chemical sort  $\alpha_j$ . This model involves seven potential functions, among which  $F_A(\bar{\rho})$  and  $F_B(\bar{\rho})$  are the embedding energy functions for atom  $A$  and  $B$ ,  $\rho_A(r)$  and  $\rho_B(r)$  are electron density functions for atom  $A$  and  $B$ ,  $\phi_{A-A}(r)$ ,  $\phi_{B-B}(r)$ , and  $\phi_{A-B}(r)$  are pair-wise interaction functions for atom  $A$ - $A$ ,  $B$ - $B$ , and  $A$ - $B$ , respectively.

In the present work, EAM potential of Mishin *et al* [13] is used which gives the value of 0.55 J/m<sup>2</sup> for the APB energy and 0.48 eV for the inter-branch-Al energy, while keeping the agreement with all other properties of B2-NiAl. Due to the comparable values of APB energy and inter-branch-Al energy with experimental data, this potential will be able to predict the more accurate phase transformation, plastic deformation and fracture properties of B2-NiAl more accurately, especially at high temperature.

The B2-NiAl nano-layer is created by generating atomic positions as in the bulk corresponding to the B2 crystal structure with known lattice constant of 0.28712 nm. The B2 structure is equivalent to a body-centered-cubic (BCC) lattice with the Ni atoms at the corners of the unit cell and a single Al atom at the body center. The B2-NiAl nanowire is first relaxed to the minimum energy configuration. After the minimization procedure, the ends of nano-layer are constrained in the <100> direction. The wires are then thermally equilibrated for a given temperature using the Nose-Hoover thermostat [14, 15] for 200 picosecond (ps) with a time step of 0.001 ps. A uniaxial tensile loading is then applied by completely restraining one end of the nano-layer, and then by applying velocity to the atoms along the loading direction, linearly from zero at the fixed end to the maximum value at the free end, thus creating a ramp velocity profile. Such a ramp velocity is used to avoid the emission of shock waves from the fixed end of the nanowire. The equations of motion are integrated in time using velocity Verlet algorithm [16]. Temperature

of the system is kept constant during the simulations, which is to capture the isothermal behavior and its effect on the phase transformation of the nano-layer. All simulations are performed using an MD code called LAMMPS [17, 18]. No periodic boundary conditions are used at any stage of simulation, which is to capture accurately the relevant surface effects. The stresses are calculated using the virial theorem [19] as

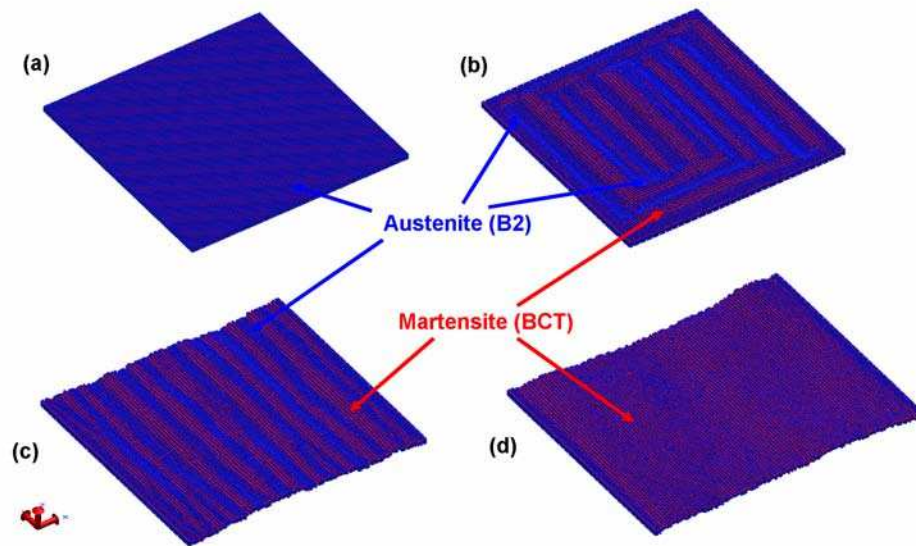
$$\sigma_{ij} = \frac{1}{V} \left( \frac{1}{2} \sum_{\alpha=1}^N \sum_{\beta \neq \alpha}^N U'(r^{\alpha\beta}) \frac{\Delta x_i^{\alpha\beta} \Delta x_j^{\alpha\beta}}{r^{\alpha\beta}} - \sum_{\alpha=1}^N m_{\alpha} \dot{x}_i^{\alpha} \dot{x}_j^{\alpha} \right), \quad (3)$$

where  $N$  is the total number of atoms,  $r^{\alpha\beta}$  is the distance between the two atoms  $\alpha$  and  $\beta$ ,  $\Delta x_i^{\alpha\beta} = x_i^{\alpha} - x_i^{\beta}$ ,  $U$  is the potential energy, and  $V$  is the volume of the nanowire for the purpose of averaging. Engineering strain is used as a measure of deformation and defined as  $\varepsilon = (l - l_0)/l_0$ , where  $l$  is the instantaneous length and  $l_0$  is the initial length of the wire obtained after the energy minimization corresponding to the initial configuration.

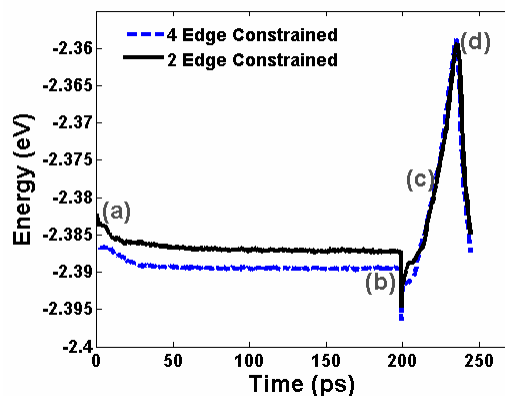
### 3. RESULTS AND DISCUSSIONS

Figure 1(a) shows the nano-layer which is first relaxed to energy minimizing positions while keeping the ends of the films free to move in all directions. It is then thermally equilibrated for a given temperature of 300K using the Nose-Hoover thermostat for 200 picoseconds (ps) with time step of 0.001 ps. Figure 1(b) shows the formation of various B2 and BCT phases after thermal equilibration without formation of any regular pattern. A uniaxial and linear ramp profile (along x-direction) of velocity is applied to the atoms with the edge ( $x=0$ ) of the nano-layer perfectly restrained. The other two parallel edges were unconstrained prior to the loading. Figure 1(c) shows the formation of wrinkle (strips) pattern of alternate B2 and BCT phases during tensile loading. Further loading causes a complete transformation into BCT phase as shown in Figure 1(d).

The effect of boundary conditions on the formation of different patterns is also analyzed. Figure 2 shows the comparison of energy between two different boundary conditions of (i) 4-edge constrained and (ii) 2-edge constrained. Lower energy of 4-edge constrained nano-layer as compared to the 2-edge constrained one is an indication that the first configuration is more stable than the second one. Further, the variation of energy with time is plotted in Figure 2, and subsequently, the deformed shape shown in Figure 1 is also marked. One can see the wrinkle pattern which is formed (as marked as (c) in Figure 2) at a higher energy level as compared to the energy of the stable phase. Also, the energy of complete transformed BCT phase shows a higher energy level, which is an indication of instability in the nano-layer.



**Figure 1.** Nano-layer of Ni-Al with an initial cross-sectional dimension of  $300 \times 300 \times 5.74 \text{ nm}^3$  (a) An initial configuration of Austenite (B2) phase after energy minimization. (b) Bands of Austenite (B2) and Martensite (BCT) phases after thermally equilibrated at 300K for 200ps. (c) Formation of wrinkled pattern (or strips) of alternate Austenite (B2) and Martensite (BCT) phases during high strain rate loading. (d) Further loading causes a complete transformation from initial Austenite (B2) to Martensite (BCT) phase.



**Figure 2.** Effect of boundary conditions on an initially Austenite (B2) Ni-Al nano-layer of size  $300 \times 300 \times 5.74 \text{ nm}^3$ .

#### 4. CONCLUSIONS

Proper tailoring of the size and thickness of nano-layers, as well as their boundary conditions can lead to a controlled surface pattern, which forms under different thermo-mechanical loadings for a range of useful nano-electro-mechanical device applications. In the present paper, the formation of different surface patterns on an initial B2-NiAl nano-layer is discussed in details. The intermediate unstable phases may be useful for various device applications where these can be controlled and switched to a stable phase by applying precise thermo-mechanical loadings.

#### REFERENCES

- [1] L. H. Nguyen, T. K. Nguyen-Duc, V. Le Thanh, F. A. d'Avitaya and J. Derrien, *Physica E (Amsterdam)* 2004, **23**, 471.
- [2] R. Hull, J. L. Gray, M. Kammler, T. Vandervelde, T. Kobayashi, P. Kumar, T. Pernell, J. C. Bean, J. A. Floro, and F. M. Ross, *Mater. Sci. Eng., B* 2003, **101**, 1.
- [3] A. Karmous, A. Cuenat, A. Ronda, I. Berbezier, S. Atha, and R. Hull, *Appl. Phys. Lett.* 2004, **85**, 6401.
- [4] G. Chen, H. Lichtenberger, F. Schaffler, G. Bauer, and W. Jantsch, *Mater. Sci. Eng., C* 2006, **26**, 795.
- [5] P. Liu, C. Lu and Y.W. Zhang, *Phys. Rev. B* 2007, **76**, 085336.
- [6] J Diao, K Gall, and M L Dunn *Nat. Mater.* 2003, **2** (10), 656-660
- [7] V K Sutrarakar and D. Roy Mahapatra *J. Phys.: Condens. Matter* 2008, **20**, 335206
- [8] V K Sutrarakar and D. Roy Mahapatra *Nanotechnology* 2009, **20**, 045701
- [9] H S Park, K Gall, and J A Zimmerman *Phys. Rev. Lett.* 2005, **95**, 255504
- [10] W Liang, M Zhou, and F Ke *Nano Lett.* 2005, **5** (10), 2039-2043
- [11] M S Daw and M I Baskes *Phys. Rev. B* 1984, **29** 6443-53
- [12] M S Daw, S M Foiles and M I Baskes *Mater. Sci. Rep.* 1993, **9** 251-310
- [13] Y Mishin, M J Mehl, and D A Papaconstantopoulos

- Phys. Rev. B* 2002, **65**, 224114
- [14] S A Nose *J Chem Phys.* 1984, **81**, 511-9
- [15] W G Hoover *Phys. Rev. A* 1985, **31**, 1695-7
- [16] W C Swope, H C Anderson, P H Berens, and K R A Wilson *J Chem Phys.* 1982, **76**, 637-649
- [17] S J Plimpton *J Comput. Phys.* 1995, **117**, 1-19
- [18] LAMMPS  
2007 <http://www.cs.sandia.gov/~sjplimp/lammps.html>
- [19] M Zhou *Proc. R. Soc. A* 2003, **459**, 2347-92

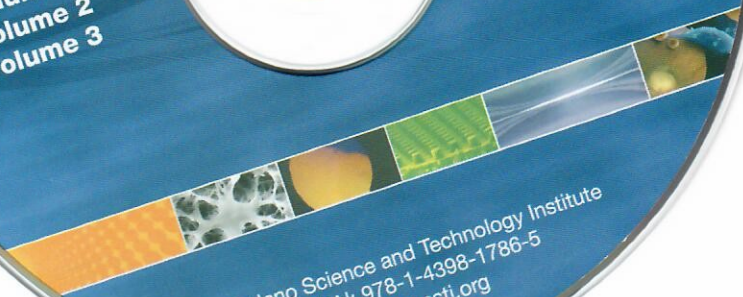
# Nanotech

Conference & Expo 2009

Technical Proceedings | Vol. 1-3

- Volume 1
- Volume 2
- Volume 3

- Indexed
- Searchable fields

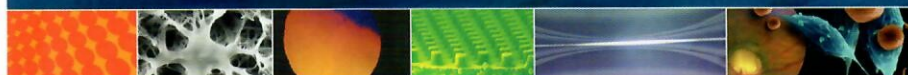


© Nano Science and Technology Institute  
ISBN: 978-1-4398-1786-5  
[www.nsti.org](http://www.nsti.org)



# Nanotech

Conference & Expo 2009



**BioNano**  
Conference & Expo 2009



**CRC** CRC Press  
Taylor & Francis Group

## Technical Proceedings | **Vol. 1-3**

**Vol. 1:** Fabrication, Particles, Characterization,  
MEMS, Electronics and Photonics

**Vol. 2:** Life Sciences, Medicine, Diagnostics,  
Bio Materials and Composites

**Vol. 3:** Biofuels, Renewable Energy, Coatings,  
Fluidics and Compact Modeling

**Vol. 1**

Nano Fabrication  
Nanoparticles  
Nanostructured Materials and Devices  
Nanoscale Characterization  
MEMS and NEMS  
Wireless MEMS  
Sensors and Systems  
Nano Electronics and Photonics

**Vol. 2**

Cancer Nanotechnology  
Drug Delivery  
Nano Medicine  
Biosensors and Diagnostics  
Bio Nano Materials  
Nano Bio Materials and Tissues  
Environment, Water, Health,  
Safety and Society  
Polymer Nanotechnology  
Nanocomposites

**Vol. 3**

Bio Energy and Bio Fuels  
Energy, Storage, Fuel Cells, Hydrogen and Grid  
Solar and PV Technologies  
Coatings and Surfaces  
Modeling and Simulation of Micro and Nano Systems  
Nanotechnology Investment and Initiatives  
Carbon Nano Structures  
Micro and Nano Fluidics  
Workshop on Compact Modeling

**CRC Press**

Taylor & Francis Group  
an informa business

[www.taylorandfrancisgroup.com](http://www.taylorandfrancisgroup.com)

6000 Broken Sound Parkway, NW  
Suite 300, Boca Raton, FL 33487  
270 Madison Avenue  
New York, NY 10016  
2 Park Square, Milton Park  
Abingdon, Oxon OX14 4RN, UK

ISBN: 978-1-4398-1786-5



9 781439 817865